

# Donor-acceptor-pair photoluminescence in Ga-doped ZnO thin films grown by plasma-assisted molecular beam epitaxy

Z. Yang and J. L. Liu<sup>a)</sup>

Department of Electrical Engineering, Quantum Structures Laboratory, University of California at Riverside, Riverside, California 92521

(Received 29 September 2009; accepted 22 February 2010; published 6 April 2010)

Three dominant emission lines: neutral Ga<sub>Zn</sub> donor bound exciton  $I_8$  (3.359 eV); ionized Ga<sub>Zn</sub> donor bound exciton  $I_1$  (3.368–3.371 eV), and donor-acceptor-pair (DAP)  $I_{DA}$  (3.313–3.321 eV) were observed in the 9 K photoluminescence (PL) spectra from a series of Ga-doped ZnO thin films with electron carrier concentration ( $n$ ) ranging from  $3.6 \times 10^{18}$  to  $3.5 \times 10^{19}$  cm<sup>-3</sup>. As  $n$  increases, the dominant PL line changes from  $I_1$  to  $I_{DA}$ , and finally to  $I_8$ . Characteristic blueshifts of  $I_{DA}$  PL lines were observed with increasing  $n$ , with increasing excitation power in power-dependent PL spectra, and with increasing temperature in temperature-dependent PL spectra. The experimental results of  $I_{DA}$  lines in Ga-doped ZnO are generalized to a proposed model to explain the possibilities of the widely observed 3.30–3.32 eV PL lines in ZnO as DAP transitions, which are associated with a shallow donor (e.g., Ga, Al, In, H, etc) with an ionization energy of  $\sim 44$ –65 meV and a deep acceptor  $V_{Zn}$  with an ionization energy of  $\sim 180$  meV. © 2010 American Vacuum Society. [DOI: 10.1116/1.3368543]

## I. INTRODUCTION

ZnO materials have potential applications in optoelectronic devices<sup>1–8</sup> and spintronics.<sup>9–12</sup> Photoluminescence (PL) properties in ZnO materials have been widely studied,<sup>1–3</sup> however, the origins of some characteristic PL lines in ZnO are not well clarified yet. For example, the origin of the PL lines located at 3.30–3.32 eV in ZnO is still controversial so far. Various assignments have been attempted for these lines,<sup>4</sup> such as acceptor-bound excitons, free electrons to neutral acceptors, and donor-acceptor pairs (DAPs). Another example is the  $I_1$  PL line in ZnO, which lies above the common neutral donor-bound-exciton lines but below the free A exciton line. The  $I_1$  line is widely observed in ZnO but its origin is also still controversial. Recently, we performed systematic PL studies in a series of Ga-doped ZnO thin films with different electron carrier concentrations ( $n$ ).<sup>5</sup> Three dominant donor-related PL lines, which are neutral Ga donor-bound-exciton  $I_8$  line (3.359 eV), ionized Ga donor-bound-exciton  $I_1$  line (3.368–3.371 eV), and DAP  $I_{DA}$  line (3.313–3.321 eV), were observed in these Ga-doped ZnO thin films.<sup>5</sup> In this paper, additional PL experimental results, including excitation power-dependent and temperature-dependent PL, are reported and analyzed to further support the DAP assignment in Ga-doped ZnO.

## II. EXPERIMENT

Ga-doped ZnO thin films were grown on *r*-plane sapphire substrates using plasma-assisted molecular beam epitaxy (MBE). Zn and Ga sources were provided by radical Zn (6N) and Ga (6N) effusion cells, and oxygen plasma was generated by a radio frequency plasma source sustained with O<sub>2</sub>

(5N) gas. O<sub>2</sub> flow rate can be precisely tuned using a mass flow controller. Sapphire substrates were cleaned by a three-step process: The first step was chemical cleaning in a hot ( $\sim 150$  °C) aqua regia (HNO<sub>3</sub>:HCl=1:3) solution for 20 min, then rinsing in de-ionized water, and finally drying with a nitrogen gun before being transferred into a MBE chamber. Next, the substrates were thermoannealed at 800 °C under vacuum for 20 min. Finally, oxygen plasma treatments were performed immediately before growth. The Ga-doped ZnO thin films were grown at 565 °C for 180 min. O<sub>2</sub> flow rate was kept at 5.0 SCCM (SCCM denotes cubic centimeter per minute at STP) for all samples. All samples were annealed *in situ* at 800 °C under vacuum for 20 min after growth. Electron carrier concentration  $n$  of the Ga-doped ZnO thin films was controlled by the amount of Ga incorporation into each film, which in turn is determined by the ratio between Ga and Zn fluxes, controlled by Ga and Zn effusion-cell temperatures. First, the Zn cell temperature was fixed at 370 °C and the Ga cell temperature was varied from 500 to 600 °C in steps of 25 °C. In this series, five Ga-doped ZnO samples, with values of  $n$  at room temperature (RT) ranging from  $5.5 \times 10^{18}$  to  $3.6 \times 10^{19}$  cm<sup>-3</sup> (samples A and C–F), were achieved. Then, a Ga-doped ZnO (sample B) with  $n=9.6 \times 10^{18}$  cm<sup>-3</sup> at RT, which is in between that of samples A and C, was grown by precisely tuning the ratio between the Zn and Ga fluxes. The detailed growth parameters of these six Ga-doped ZnO thin film samples are summarized in Table I.

Photoluminescence measurements were carried out using a home-built PL system. The 325 nm wavelength He–Cd laser was used as an excitation source and a photomultiplier tube was used to detect the PL signals. The resolution of the PL system was 0.15 nm, which is  $\sim 1.5$  meV in the ultraviolet emission region. The temperature control from 9 to 300 K in the PL system was achieved using a Janis Cryostat

<sup>a)</sup> Author to whom correspondence should be addressed; electronic mail: jianlin@ee.ucr.edu

TABLE I. Growth parameters and electron carrier concentrations at 300 K ( $n_{300\text{ K}}$ ) and 10 K ( $n_{10\text{ K}}$ ) of Ga-doped ZnO thin film samples A–F.

| Sample | $T_{\text{Zn}}^{\text{a}}$<br>(°C) | $T_{\text{Ga}}^{\text{b}}$<br>(°C) | $F_{\text{O}_2}^{\text{c}}$<br>(SCCM) | $n_{300\text{ K}}$<br>( $\text{cm}^{-3}$ ) | $n_{10\text{ K}}$<br>( $\text{cm}^{-3}$ ) |
|--------|------------------------------------|------------------------------------|---------------------------------------|--|---|
| A      | 370                                | 500                                | 5.0                                   | $5.5 \times 10^{18}$                       | $3.6 \times 10^{18}$                      |
| B      | ~360                               | 500                                | 5.0                                   | $9.6 \times 10^{18}$                       | $8.8 \times 10^{18}$                      |
| C      | 370                                | 525                                | 5.0                                   | $1.5 \times 10^{19}$                       | $1.5 \times 10^{19}$                      |
| D      | 370                                | 550                                | 5.0                                   | $2.3 \times 10^{19}$                       | $2.2 \times 10^{19}$                      |
| E      | 370                                | 575                                | 5.0                                   | $2.5 \times 10^{19}$                       | $2.4 \times 10^{19}$                      |
| F      | 370                                | 600                                | 5.0                                   | $3.6 \times 10^{19}$                       | $3.5 \times 10^{19}$                      |

<sup>a</sup> $T_{\text{Zn}}$ : Zn effusion cell temperature.<sup>b</sup> $T_{\text{Ga}}$ : Ga effusion cell temperature.<sup>c</sup> $F_{\text{O}_2}$ : O<sub>2</sub> flow rate.

equipped with a He compressor. Various excitation powers were achieved by filtering the excitation laser beam. Hall-effect measurements were carried out using a Quantum Design physical properties measurement system in Hall bar geometry at 10 and 300 K with various magnetic fields (1–10 T). The room-temperature Hall-effect data were further crosschecked using an Ecopia HMS-3000 Hall effect measurement system in Van der Pauw geometry at 1 T magnetic field. The 300 and 10 K  $n$  values of the samples are shown in Table I. The  $n$  values do not show strong temperature dependence, since they are basically degenerate.

### III. RESULTS AND DISCUSSION

Three dominate PL lines, labeled as  $I_1$ ,  $I_8$ , and  $I_{DA}$  are observed in the 9 K PL spectra of Ga-doped ZnO thin film samples A–F in Fig. 1, with  $I_1$  at 3.368–3.371 eV in samples A–D;  $I_8$  at 3.359 eV in samples E–F; and  $I_{DA}$  at 3.313–3.321 eV in samples A–F. As  $n$  increases from  $3.6 \times 10^{18}$  to  $3.5 \times 10^{19} \text{ cm}^{-3}$ , the dominant PL line in Ga-doped ZnO changes from  $I_1$  to  $I_{DA}$ , and finally to  $I_8$ .

The  $I_8$  line is the commonly accepted and almost universally acknowledged to be a neutral  $\text{Ga}_{\text{Zn}}$  donor-bound-exciton ( $D^0, X$ ) recombination.<sup>2,13–19</sup> The  $I_1$  line lies above the common neutral donor-bound-exciton lines,  $I_9(\text{In})$ ,  $I_8(\text{Ga})$ ,  $I_6(\text{Al})$ , and  $I_4(\text{H})$ , which span the range of 3.357–3.363 eV, but below the free A exciton line at 3.377 eV. It has been seen in the past<sup>1,2</sup> and recently it has been assigned as an exciton bound to an ionized Ga donor ( $D^+, X$ ).<sup>5,15,16</sup> The existence of ( $D^+, X$ ) in Ga-doped ZnO and dominance of ( $D^+, X$ ) in low-Ga-doped ZnO have been explained elsewhere.<sup>5,20</sup> The  $I_{DA}$  lines in the region 3.313–3.321 eV were assigned as DAP transitions,<sup>5</sup> consisting of transitions between neutral  $\text{Ga}_{\text{Zn}}$  donors with  $E_D(\text{Ga}_{\text{Zn}}) = 55 \text{ meV}$ ,<sup>2,14</sup> and neutral Zn-vacancy ( $V_{\text{Zn}}$ ) acceptors<sup>21</sup> with  $E_A(V_{\text{Zn}}) = 180 \text{ meV}$  based on density functional theory calculations.<sup>22</sup>

Figure 2 shows the relation between the  $I_{DA}$  PL line position and the electron carrier concentration in the samples. It is observed that the  $I_{DA}$  blueshifts from 3.313 eV in sample A to 3.321 eV in samples D–F with increasing Ga donor concentrations, which is a typical characteristic of DAP,<sup>23–25</sup> because the average donor-acceptor separation decreases with

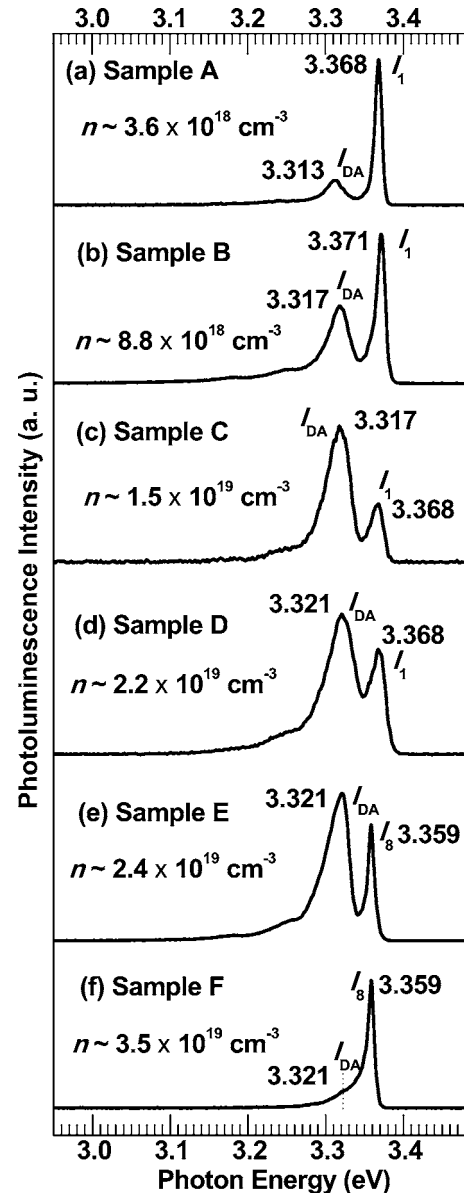


Fig. 1. PL spectra measured at 9 K for samples A–F [(a)–(f)].

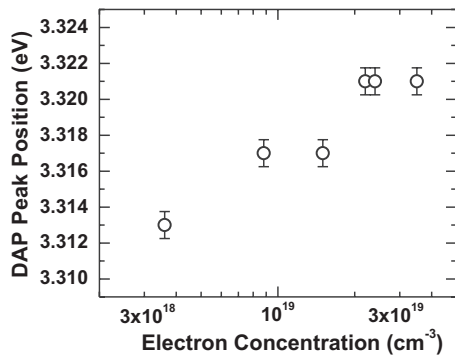


FIG. 2. DAP PL lines position with different electron carrier concentration in samples A–F. The error bars in the graph represent the resolution ( $\sim 1.5$  meV) of the PL system.

increased donor concentration and consequently the DAP lines shift to higher energy. This characteristic of DAP were also observed in other II–VI and III–V semiconductors.<sup>23–25</sup> The error bars in Fig. 2 represent the resolution ( $\sim 1.5$  meV) of the PL system.

Figures 3(a) and 3(b) show the excitation power-dependent PL performed at 9 K on samples D and E. The behaviors on power dependence of all three characteristic PL lines ( $I_{DA}$ ,  $I_1$ , and  $I_8$ ) in the Ga-doped ZnO samples are included. The  $I_{DA}$  transition energy clearly blueshifts with increased excitation power, whereas those of  $I_1$  and  $I_8$  do not. This is a strong indication that  $I_{DA}$  represents a DAP transition. The average donor-acceptor separation decreases when

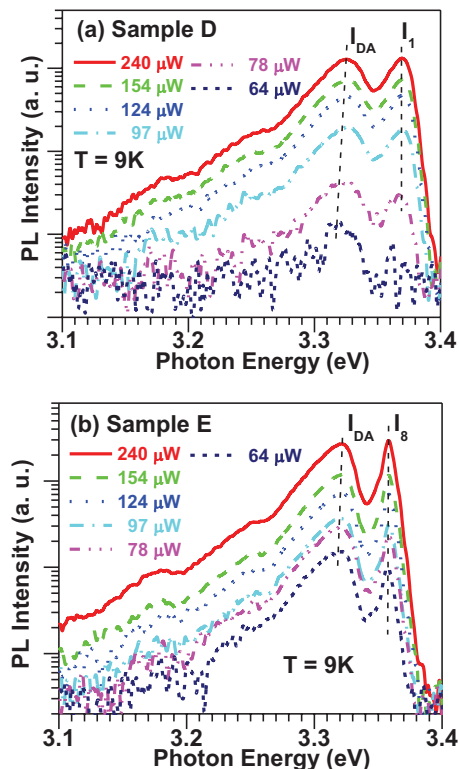


FIG. 3. (Color online) Excitation power-dependent PL spectra of samples (a) D and (b) E at 9 K.

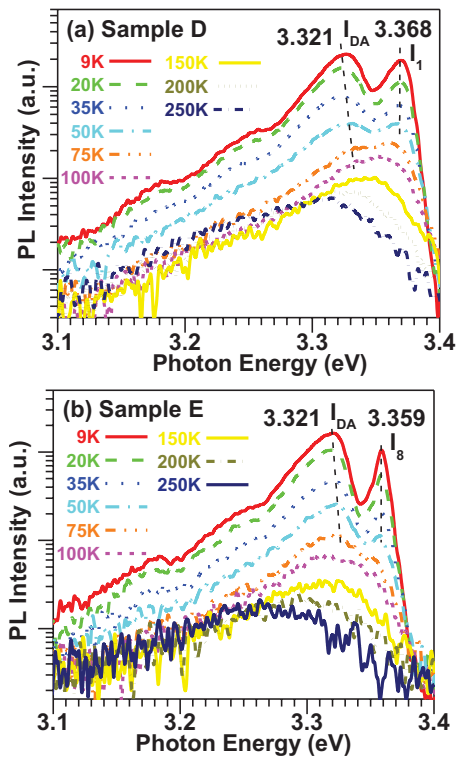


FIG. 4. (Color online) Temperature-dependent PL spectra of samples (a) D and (b) E at 9 K.

the excitation power intensity increases due to the increasing amount of photoexcited DAPs.<sup>23,24,26</sup> The blueshifted values in samples D and E are small (especially in sample E), which is due to the relatively small variation range of the excitation power (less than 4 times the difference from 64 to 240  $\mu\text{W}$ ).

Figures 4(a) and 4(b) show temperature-dependent PL spectra of samples D and E. As temperature increases, a DAP transition energy might be expected to shift in two different ways: (1) a blueshift due to the donor electron first being thermally excited to the conduction band (CB) before its radiative capture by the acceptor; and (2) a redshift due to band gap shrinkage. At a given temperature, a fraction of the donor electrons in the DAPs will have been thermally excited to the CB before being captured by their paired acceptors, and those electrons will thus recombine with an energy higher by about 55 meV, the donor energy. The overall blueshift might then be expected to be about 55 meV. On the other hand, the CB itself will have shifted downwards, leading to a redshift. The two effects will partially cancel each other, so the overall effect could be small. As seen in Fig. 4, from about 9–150 K, the  $I_{DA}$  peak energy shows a blueshift  $\leq 20$  meV with increasing temperature in sample D, and an even smaller shift in sample E. Even though quantitative analysis is difficult with such small shifts, the qualitative behavior of  $I_{DA}$  is consistent with a DAP recombination model.

Based on the analyses of  $I_{DA}$  PL lines in Ga-doped ZnO, a more generalized model is proposed here as a possible explanation for the widely observed 3.30–3.32 eV PL lines in ZnO materials. In this model, the 3.30–3.32 eV PL lines are

proposed to be associated with DAP transitions in ZnO. The energy of a DAP transition can be expressed as

$$E_{DA} = E_g - E_D(\text{Ga}_{\text{Zn}}^{0/+}) - E_A(\text{V}_{\text{Zn}}^{0/-}) + e^2/4\pi\epsilon r_{DA} - E_{\text{vdW}}, \quad (1)$$

where  $E_g$  is the ZnO band gap of  $\sim 3.437$  eV ( $< 10$  K),  $E_D$  is the donor ionization energy, and  $E_A$  is the acceptor ionization energy. The donor could be not only Ga but also any shallow donors (e.g., Al, In, H, etc., with ionization energies in range of 44–65 meV). The acceptor could be  $\text{V}_{\text{Zn}}$ , a deep acceptor with an ionization energy of  $\sim 180$  meV,<sup>22</sup> which is also common in  $n$ -type ZnO due to its low formation energy.<sup>21</sup> The Coulomb energy  $e^2/4\pi\epsilon r_{DA}$  is approximately estimated by the carrier density  $n$  with

$$r_{DA} \approx \left( \frac{3}{4\pi n} \right)^{1/3},$$

which is  $\sim 40$ – $150$  meV with  $n$  ranging from  $3 \times 10^{18}$  to  $1 \times 10^{20}$   $\text{cm}^{-3}$ . The  $E_{\text{vdW}}$  is the van der Waals (vdW) polarization energy, which generally is small and can be neglected unless  $r_{DA}$  is smaller than 2 nm (e.g.,  $E_{\text{vdW}} \sim 14$  meV as  $r_{DA} \sim 1$  nm).<sup>5</sup> Using these numbers into Eq. (1), it supports the above proposed generalized model of the DAP explanation for the widely observed 3.30–3.32 eV PL emissions in different kinds of undoped and doped ZnO materials.

#### IV. SUMMARY

In summary, Ga-doped ZnO thin films with electron carrier concentrations (at 10 K) from  $3.6 \times 10^{18}$  to  $3.5 \times 10^{19}$   $\text{cm}^{-3}$  were grown by plasma-assisted molecular beam epitaxy. The 9 K PL spectra are dominated by three lines: neutral  $\text{Ga}_{\text{Zn}}$  bound exciton  $I_8$  at 3.359 eV; ionized  $\text{Ga}_{\text{Zn}}$  bound exciton  $I_1$  at 3.368–3.371 eV; and DAP  $I_{DA}$  at 3.313–3.321 eV. The dominant PL peak evolves from  $I_1$  to  $I_{DA}$ , and finally to  $I_8$ , with increasing electron carrier concentration. Blueshifts of the  $I_{DA}$  lines were observed with increasing electron carrier concentration, with increasing excitation power in power-dependent PL, and with increasing temperature in temperature-dependent PL, which all support DAP assignments. A generalized model is proposed to explain the 3.30–3.32 eV PL lines in ZnO, which are associated with a

shallow donor (e.g., Ga, Al, In, H, etc.) with an ionization energy of  $\sim 44$ – $65$  meV and a deep acceptor  $\text{V}_{\text{Zn}}$  with an ionization energy of  $\sim 180$  meV.

#### ACKNOWLEDGMENTS

This work was in part supported by NSF (Grant No. ECCS-0900978) and DMEA through the Center of Nanomaterials and Nanodevice (CNN) under the Grant No. H94003-08-2-0803. The authors also would like to thank useful discussions with Professor David Look of Semiconductor Research Center, Wright State University, Dayton, OH.

<sup>1</sup>D. C. Reynolds, C. W. Litton, and T. C. Collins, Phys. Rev. **140**, A1726 (1965).

<sup>2</sup>B. K. Meyer *et al.*, Phys. Status Solidi B **241**, 231 (2004).

<sup>3</sup>Ü. Özgür *et al.*, J. Appl. Phys. **98**, 041301 (2005).

<sup>4</sup>M. Schirra *et al.*, Phys. Rev. B **77**, 125215 (2008).

<sup>5</sup>Z. Yang, D. C. Look, and J. L. Liu, Appl. Phys. Lett. **94**, 072101 (2009).

<sup>6</sup>L. J. Mandalapu, Z. Yang, F. X. Xiu, D. T. Zhao, and J. L. Liu, Appl. Phys. Lett. **88**, 092103 (2006).

<sup>7</sup>S. Chu, J. H. Lim, L. J. Mandalapu, Z. Yang, L. Li, and J. L. Liu, Appl. Phys. Lett. **92**, 152103 (2008).

<sup>8</sup>S. Chu, M. Olmedo, Z. Yang, J. Kong, and J. L. Liu, Appl. Phys. Lett. **93**, 181106 (2008).

<sup>9</sup>Z. Yang, J. L. Liu, M. Biasini, and W. P. Beyermann, Appl. Phys. Lett. **92**, 042111 (2008).

<sup>10</sup>Z. Yang *et al.*, J. Appl. Phys. **104**, 113712 (2008).

<sup>11</sup>Z. Yang *et al.*, J. Appl. Phys. **105**, 053708, (2009).

<sup>12</sup>C. Liu, F. Yun, and H. Morkoç, J. Mater. Sci.: Mater. Electron. **16**, 555 (2005).

<sup>13</sup>H. J. Ko, Y. F. Chen, S. K. Hong, H. Wensch, T. Yao, and D. C. Look, Appl. Phys. Lett. **77**, 3761 (2000).

<sup>14</sup>D. C. Look, G. C. Farlow, P. Reunchan, S. Limpijumnong, S. B. Zhang, and K. Nordlund, Phys. Rev. Lett. **95**, 225502 (2005).

<sup>15</sup>F. Bertram, J. Christen, A. Dadgar, and A. Krost, Appl. Phys. Lett. **90**, 041917 (2007).

<sup>16</sup>B. K. Meyer, J. Sann, S. Lautenschläger, M. R. Wagner, and A. Hoffmann, Phys. Rev. B **76**, 184120 (2007).

<sup>17</sup>H. C. Park, D. Byun, B. Angadi, D. H. Park, W. K. Choi, J. W. Choi, and Y. S. Jung, J. Appl. Phys. **102**, 073114 (2007).

<sup>18</sup>D. Weissenberger *et al.*, Appl. Phys. Lett. **91**, 132110 (2007).

<sup>19</sup>R. Schneider *et al.*, Appl. Phys. Lett. **92**, 131905 (2008).

<sup>20</sup>D. C. Look, J. Appl. Phys. **104**, 063718 (2008).

<sup>21</sup>F. Tuomisto, V. Ranki, K. Saarinen, and D. C. Look, Phys. Rev. Lett. **91**, 205502 (2003).

<sup>22</sup>A. Janotti and C. G. Van de Walle, Phys. Rev. B **76**, 165202 (2007).

<sup>23</sup>P. J. Dean, Prog. Solid State Chem. **8**, 1 (1973).

<sup>24</sup>G. D. Gilliland, Mater. Sci. Technol. **18**, 99 (1994).

<sup>25</sup>E. H. Bogardus and H. Bebb, Phys. Rev. **176**, 993 (1968).

<sup>26</sup>K. Tamura *et al.*, Solid State Commun. **127**, 265 (2003).